ISCI, Volume *23*

Supplemental Information

System-Level Analysis of Lignin Valorization in Lignocellulosic Biorefineries

Kefeng Huang, Peyman Fasahati, and Christos T. Maravelias

Supplemental Figures

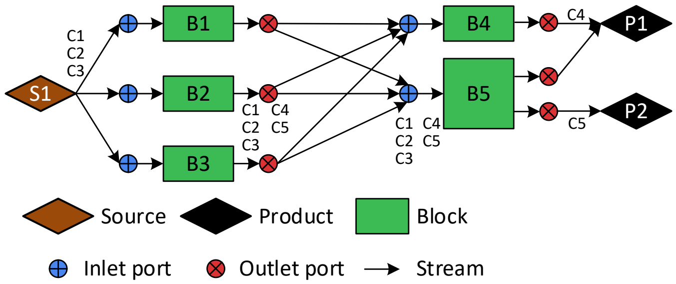

Figure S1. Representation of a general superstructure. B1 – B5 are blocks; C1 – C5 are components; SR1 and P1 – P2 are source and products, Related to **Figure 1**.

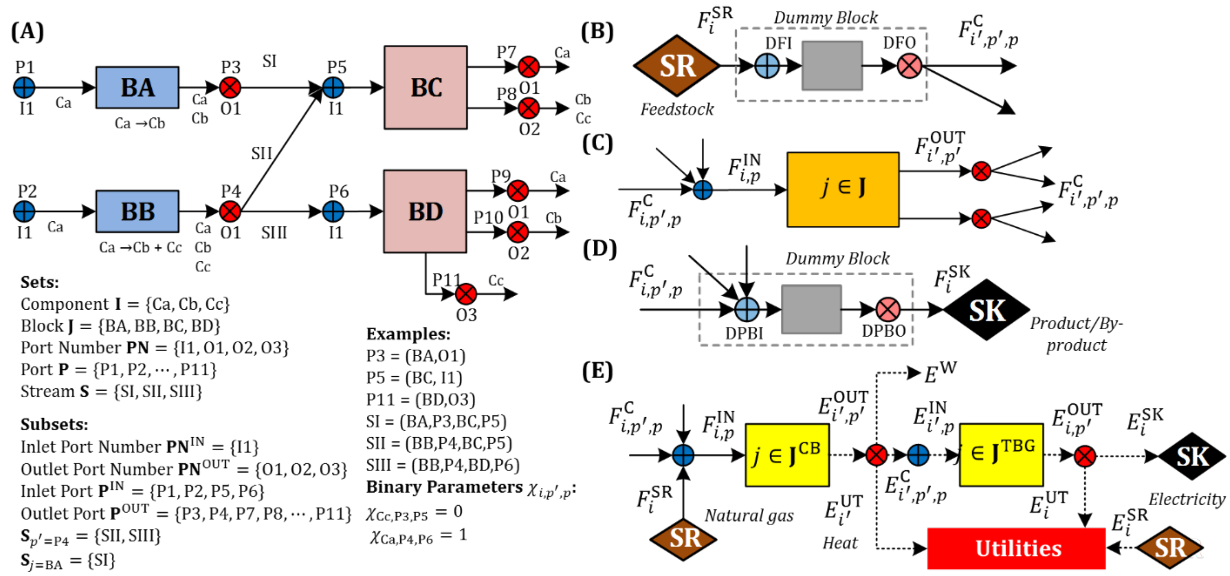

Figure S2. (A) Example of sets, subsets and binary parameters. (B) – (E) Generic mass and energy flow, Related to **Figure 1**.

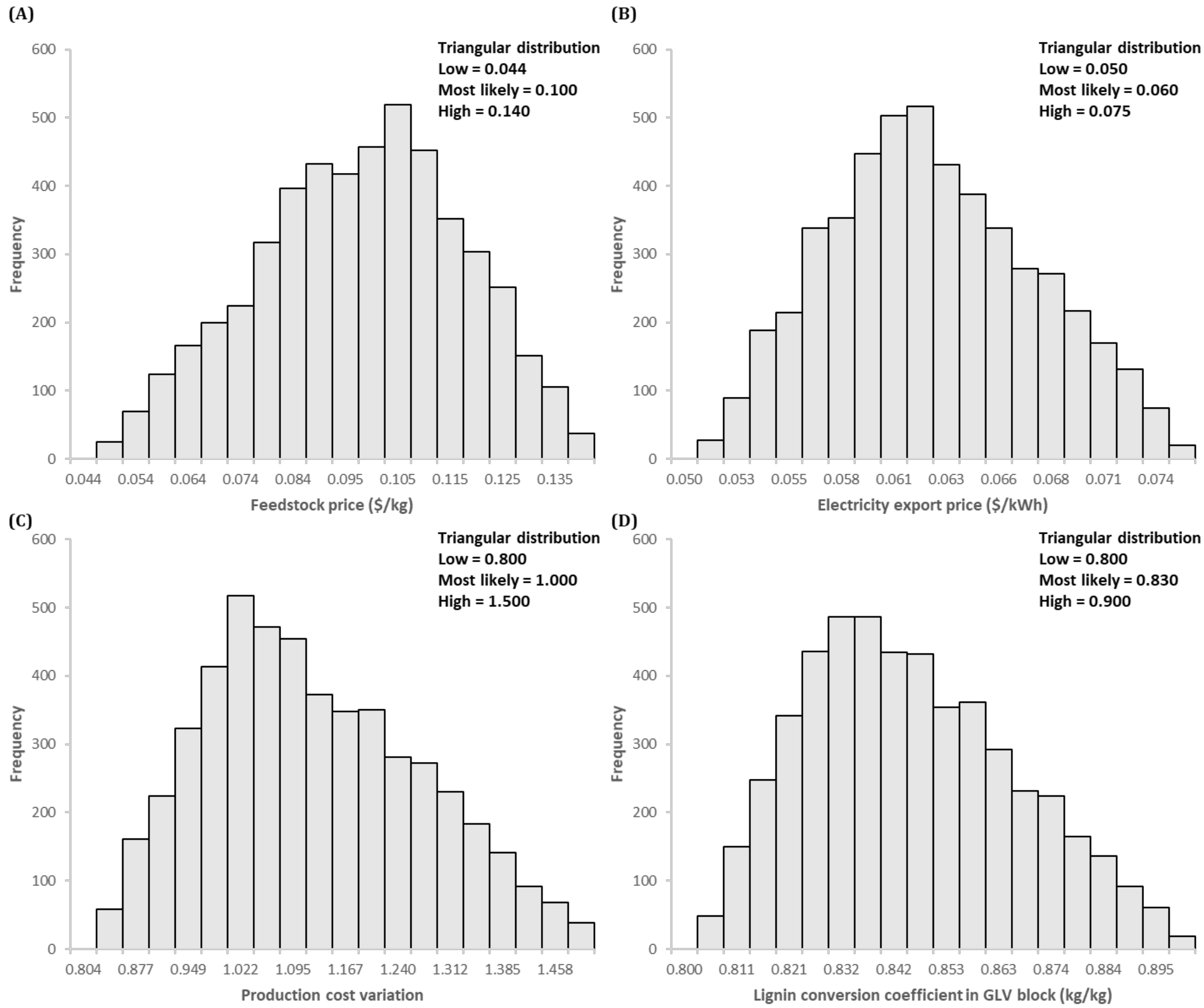

Figure S3. Histograms of values of parameters used for the assessment of the impact of uncertainty on the ethanol cost of the base case strategy. (A) Feedstock price, (B) Electricity export price, (C) Production cost variation, and (D) Lignin conversion coefficient in GVL block. Note that production cost variation is used as a multiplier to the sum of the production costs of all process blocks, Related to **Figure 2**.

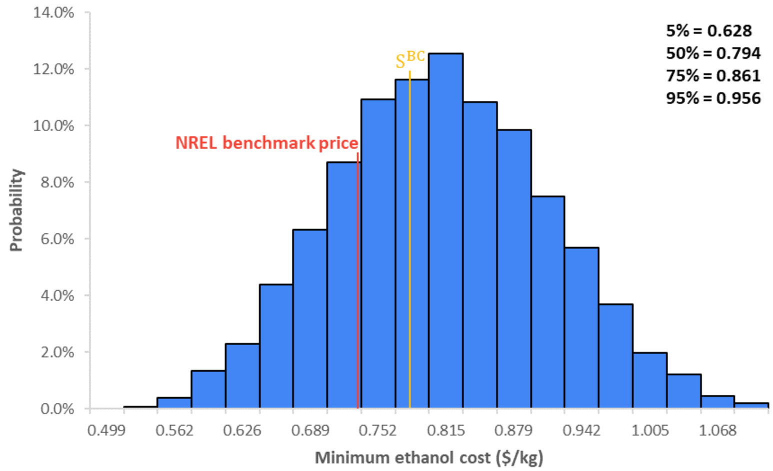

Figure S4. Distribution of the minimum ethanol cost of the base case in the scenarios generated by varying the values of four key parameters not directly related to lignin valorization (histograms of values shown in **Figure S3**), Related to **Figure 2.**

Supplemental Tables

Table S1. Composition of feedstock and unit price of components, Related to **Figure 1**.

Item	Value
Composition of Corn Stover	
Glucan	0.496
Xylan	0.293
Lignin	0.211
Unit Price λ_i (\$ kg^{-1} or *\$ kWh^{-1})	
Corn Stover	0.100
Natural Gas (purchase)	0.600
Electricity (export)	0.060*
Electricity (purchase)	0.065*
Bioproducts (SV)	2.000
Bioproducts (LV)	1.000

Table S2. Conversion coefficient of each block, Related to **Figure 1.**

i	i'	j	pn	pn	$\eta_{i,p,i',p'}$
Glucan	Glucose	DA	I1	O1	0.111
Glucan	Glucan	DA	I1	O1	0.900
Xylan	Xylose	DA	I1	O1	1.023
Xylan	Xylan	DA	I1	O1	0.100
Lignin	Lignin	DA	I1	O1	0.950
Glucan	Glucose	HYD1	I1	O1	1.000
Glucan	Glucan	HYD1	I1	O1	0.100
Xylan	Xylan	HYD1	I1	O1	1.000
Glucose	Glucose	HYD1	I1	O1	0.891
Xylose	Xylose	HYD1	I1	O1	0.871
Lignin	Lignin	HYD1	I1	O1	1.000
Glucose	Ethanol	COFER1	I1	O1	0.486
Xylose	Ethanol	COFER1	I1	O1	0.434
Glucose	Glucose	COFER1	I1	O1	0.050
Xylose	Xylose	COFER1	I1	O1	0.150
Glucan	Glucan	COFER1	I1	O1	0.990
Xylan	Xylan	COFER1	I1	O1	0.990
Lignin	Lignin	COFER1	I1	O1	1.000
Glucose	Ethanol	SSCF	I1	O1	0.350
Xylose	Ethanol	SSCF	I1	O1	0.330
Glucan	Ethanol	SSCF	I1	O1	0.510
Glucan	Glucose	SSCF	I1	O1	0.060
Xylose	Xylose	SSCF	I1	O1	0.150

Table S2 (continued)**.** Conversion coefficient of each block, Related to **Figure 1.**

i	i'	j	pn	pn	$\eta_{i,p,i',p'}$
Glucan	Glucan	SSCF	I1	O1	0.089
Xylan	Xylan	SSCF	I1	O1	0.990
Lignin	Lignin	SSCF	I1	O1	1.000
Ethanol	Ethanol	SEP1	I1	O1	0.950
Glucose	Glucose	SEP1	I1	O2	1.000
Xylose	Xylose	SEP1	I1	O2	1.000
Glucan	Glucan	SEP1	I1	O3	1.000
Xylan	Xylan	SEP1	I1	O3	1.000
Lignin	Lignin	SEP1	I1	O3	1.000
Glucose	Bioproducts (SV)	SV	I1	O1	0.300
Glucose	Glucose	SV	I1	O2	0.700
Xylose	Bioproducts (SV)	SV	I1	O1	0.300
Xylose	Xylose	SV	I1	O2	0.700
Glucose	Biogas	WWT	I1	O1	0.267
Xylose	Biogas	WWT	I1	O1	0.733
Biogas	Heat	CB	I1	O1	16.670
Glucan	Heat	CB	I1	O1	7.580
Xylan	Heat	CB	I1	O1	7.580
Lignin	Heat	CB	I1	O1	8.200
Lignin	Bioproducts (LV)	LV	I1	O1	0.300
Lignin	Lignin	LV	I1	O2	0.700
Glucan	Glucan	LV	I1	O2	1.000
Xylan	Xylan	LV	I1	O2	1.000
Glucan	Glucan	AFEX	I1	O1	0.950
Xylan	Xylan	AFEX	I1	O1	0.950
Lignin	Lignin	AFEX	I1	O1	0.950
Glucan	Glucose	HYD2	I1	O1	0.800
Glucan	Glucan	HYD2	I1	O1	0.100
Xylan	Xylan	HYD2	I1	O1	0.100
Xylan	Xylose	HYD2	I1	O1	0.795
Lignin	Lignin	HYD2	I1	O1	1.000
Heat	Electricity	TBG	I1	O1	0.750
Natural Gas	Heat	CB	I1	O1	13.880
Lignin	Lignin	AHP	I1	O1	0.784
Glucan	Glucan	AHP	I1	O2	0.950
Xylan	Xylan	AHP	I1	O2	0.548
Glucan	DGlucan	AHP	I1	O2	0.050
Xylan	DXylan	AHP	I1	O2	0.453
Lignin	Lignin	AHP	I1	O2	0.216

Table S2 (continued)**.** Conversion coefficient of each block, Related to **Figure 1.**

i	*i′*	*j*	*pn*	*pn*	$\eta_{i,p,i',p'}$
Glucan	Glucose	HYD3	I1	O1	1.089
Xylan	Xylose	HYD3	I1	O1	1.057
DGlucan	Glucose	HYD3	I1	O1	1.111
DXylan	Xylose	HYD3	I1	O1	1.136
Lignin	Lignin	HYD3	I1	O1	1.000
Glucan	Glucan	HYD3	I1	O1	0.010
Xylan	Xylan	HYD3	I1	O1	0.050
Lignin	Lignin	EA	I1	O1	0.440
Glucan	Glucan	EA	I1	O2	0.960
Xylan	Xylan	EA	I1	O2	0.960
Glucan	DGlucan	EA	I1	O2	0.040
Xylan	DXylan	EA	I1	O2	0.040
Lignin	Lignin	EA	I1	O2	0.560
Glucan	Glucose	HYD4	I1	O1	1.044
Xylan	Xylose	HYD4	I1	O1	0.966
DGlucan	Glucose	HYD4	I1	O1	1.111
DXylan	Xylose	HYD4	I1	O1	1.136
Lignin	Lignin	HYD4	I1	O1	1.000
Glucan	Glucan	HYD4	I1	O1	0.060
Xylan	Xylan	HYD4	I1	O1	0.150
Lignin	Lignin	GVL	I1	O1	0.830
Glucan	Glucan	GVL	I1	O1	0.120
Xylan	Xylan	GVL	I1	O1	0.170
Glucan	Glucose	GVL	I1	O2	0.800
Xylan	Xylose	GVL	I1	O2	0.750
Glucose	Glucose	COFER2	I1	O1	0.130
Xylose	Xylose	COFER2	I1	O1	0.130
Glucose	Ethanol	COFER2	I1	O1	0.485
Xylose	Ethanol	COFER2	I1	O1	0.485
Glucose	Glucose	SEP2	I1	O2	1.000
Xylose	Xylose	SEP2	I1	O2	1.000
Ethanol	Ethanol	SEP2	I1	O1	0.990

Table S3. Unit heat and electricity requirement, and unit production cost of different blocks, Related to **Figure 1.**

Block	Heat $\mu_{i=\text{heat},j}$ (kWh kg-1)	Electricity $\mu_{i=\text{electricity},j}$ (kWh kg-1)	Production Cost θ_j (\$ kg-1 or *\$ kWh-1)	Reference
DA	0.737	0.086	0.050	Humbird et al., 2011
AFEX	0.664	0.090	0.030	Kazi et al., 2010
HYD1	0.008	0.080	0.044	Humbird et al., 2011
HYD2	0.020	0.120	0.044	Kazi et al., 2010
SSCF	0.008	0.142	0.028	Aden et al., 2002
COFER1	-	0.045	0.060	Humbird et al., 2011
SEP1	1.050	0.054	0.025	Humbird et al., 2011
WWT	0.004	1.830	0.400	Humbird et al., 2011
LV	2.700	0.050	0.162	Ng et al., 2019
CB	-	0.058	0.060	Humbird et al., 2011
TBG	-	-	0.008*	Humbird et al., 2011
EA	2.447	0.138	0.040	Da Costa Sousa et al., 2016
AHP	0.250	0.040	0.219	Bhalla et al., 2018
HYD3	0.008	0.091	0.046	Bhalla et al., 2018
HYD4	0.008	0.091	0.046	Bhalla et al., 2018
SEP2	0.500	0.030	0.020	Won et al., 2017
COFER2	0.555	0.030	0.045	Won et al., 2017
GVL	1.000	0.080	0.051	Won et al., 2017
SV	5.000	0.060	0.600	Ng et al., 2019

Transparent Methods

Optimization-based Process Synthesis

Optimization-based synthesis involves three major steps: (1) constructing a superstructure with possible process alternatives, (2) formulating an optimization model representing mass and energy balances of the underlying systems, and (3) solving the resulting model to determine the optimal configuration and processing conditions (Wu et al., 2016). Consider a generic superstructure (**see Figure S1**) consisting of four major elements:

(1) Block: has one or more operations/technologies (e.g., fermentation, hydrolysis, separation, etc).
(2) Port: corresponds to stream inlet/outlet point of each block. An inlet port merges substreams from different outlet ports into a parent stream for entering a block, while an outlet port splits the parent stream leaving a block into substreams that flow to different inlet ports (Wu et al., 2016). In particular, a block can have multiple outlet port, but only one inlet port.
(3) Stream: connects an outlet and inlet port.
(4) Component: consists of all chemical components to be included in the studied process. The component flow is carried by each stream.

In this work, each block has a set of technical (conversion coefficient), economic (unit conversion cost), and energy (heat and electricity requirement) parameters, which are obtained from the literature or using simple process models (see the details in the next section "Parameter Determination"). Note that the unit conversion cost has capital, fixed and variable operating cost components. Lower and upper capacity bounds are also defined. For sources and sinks, we obtain the components' unit prices, as well as their minimum and maximum supplies or demands.

Parameter Determination

We first assume the market price of feedstocks, resources, products, and by-products can be found from literature (Bhalla et al., 2018; da Costa Sousa et al., 2016; Humbird et al., 2011; Kazi et al., 2010; Ng et al., 2019; US Environmental Protection Agency, 2018; Won et al., 2017) (**Table S1**). All costs are indexed to 2017 US dollars and calculated based on a dry mass basis.

Next, we calculate conversion coefficients based on the components exist in the inlet and outlet flows of the block (**Table S2**). Note that auxiliary inputs (e.g., water, catalyst, enzymes, etc.) do not appear as components in the superstructure, thus they are not included in the calculation of conversion coefficients (see (Kim et al., 2013) for more details). The unit energy consumption of each block (**Table S2**) is calculated based on the total annual energy divided by the annual consumption rate (exclude auxiliary inputs) of the block. The boiler efficiency is assumed as 80%.

We also calculate the unit production cost (**Table S3**), which has capital, fixed and variable operating cost components. The capital cost includes the costs of equipment and other miscellaneous costs, e.g., piping and instrumentation, etc. (Humbird et al., 2011). The annualized capital cost is then calculated from the capital multiplied by the capital recovery factor based on 10% of interest rates and 25 years of plant's lifetime. The fixed operating cost includes labor charges, maintenance, etc., while the variable operating cost covers material purchase, waste handling, etc. Auxiliary inputs (e.g., water, catalyst, enzymes, etc.) are included in the calculation of operating costs. The unit production cost is calculated based on the summation of annual operating costs and annualized capital cost, divided by the annual consumption rate of the block (see (Kim et al., 2013) for more details).

Problem Statement

We consider a problem with given biomass feedstock (e.g., corn stover, switch grass or pinewood), intermediates (glucose, xylose, and lignin), products (e.g., ethanol, bioproducts, and electricity), as well as external resources (e.g., natural gas and electricity) which are available to purchase if needed. The unit prices of biomass feedstock, products, by-products, and external resources are known. A set of blocks (pretreatment, hydrolysis, fermentation, separation, heat and power generation, etc.) are defined to convert biomass feedstock into ethanol, by-products, and energy. Each block has known energy requirement, conversion efficient, and unit conversion cost. In addition, the lower and upper bounds for (1) capacity of the block, (2) biomass feedstock availability and external resource supplies, and (3) product and by-product demands are also predetermined. We aim to identify the least cost strategy to produce one kg of ethanol. The optimization model has decision variables, such as the material and energy flow of each block, the feedstock and external resources purchase, and the by-product sales.

Biorefinery Superstructure

Figure 1 shows the superstructure for the conversion of corn stover to ethanol (Ng et al., 2019). The corn stover feedstock, consisting of glucan, xylan, and lignin, can be sent to five candidate pretreatment blocks (e.g., dilute acid-based (DA), ammonia fiber expansion-based (AFEX), copper-catalyzed alkaline hydrogen peroxide-based (AHP) (Bhalla et al., 2018), extractive ammonia-based (EA), and γ-valerolactone-based (GVL)). The effluent of the pretreatment block is fed to corresponding hydrolysis and fermentation blocks (e.g., simultaneous saccharification and co-fermentation (SSCF), co-fermentation (COFER1)), to produce sugars (e.g., glucose and xylose) from glucan and xylan. The produced sugars are converted to ethanol. Ethanol is then recovered from water, stillage (glucose and xylose), and solid residues in the separation block (SEP1).

Stillage can be utilized either in the valorization block (SV) to produce and recover value-added bioproducts or in the wastewater treatment block (WWT) to produce biogas. Similarly, solid residues (mainly lignin) can be valorized (LV) to produce value-added bioproducts and/or combusted with biogas from SV in the combustor and boiler (CB) to generate heat. Excessive heat is used to generate electricity in the turbogenerator (TBG). External resources (e.g., natural gas, electricity, etc.) can be purchased if the generated heat and power are not sufficient (i.e., the biorefinery is "energy-deficient".) to satisfy the energy requirement in the biorefinery. Note that both SV and LV blocks have considered the units required for the separation and recovery of high purity bioproducts.

The GVL block includes both conversion and separation; and has two outlet streams: sugars and solid residues. The former is sent to co-fermentation (COFER2) and the subsequent separation (SEP2) directly, while the latter is sent for lignin valorization (LV) and/or heat generation (CB).

All parameter data are provided in the Supplementary Material. All costs are indexed to 2017 US dollars and calculated based on a dry mass basis. The objective function is to minimize the total cost to produce 1 kg of ethanol, which includes the feedstock and additional resource purchases, and the production costs, minus the sales of by-products. Thus, the minimum ethanol cost is equivalent to the minimum ethanol selling price (MESP, the breakeven selling price that leads to zero net present value). The mixed-integer linear programming (MINLP) model is subject to material and energy balance, and constraints that are presented in Supplemental Material. We use GAMS 25.1 with BARON as the global MINLP solver.

Mathematical Formulation

Formally, the problem is stated in terms of the following sets and subsets:

a) Components $i \in \mathbf{I}$.
   - $\mathbf{I}^{\mathrm{F}}$: biomass feedstocks; $\mathbf{I}^{\mathrm{R}}$: resources; $\mathbf{I}^{\mathrm{I}}$: intermediates; $\mathbf{I}^{\mathrm{E}}$: energy; $\mathbf{I}^{\mathrm{P}}$: products; $\mathbf{I}^{\mathrm{B}}$: by-products.

b) Blocks $j \in \mathbf{J}$.
   - $\mathbf{J}^{\mathrm{PRE}}$: pretreatment; $\mathbf{J}^{\mathrm{HYD}}$ = hydrolysis; $\mathbf{J}^{\mathrm{FER}}$ = fermentation; $\mathbf{J}^{\mathrm{SEP}}$ = separation; $\mathbf{J}^{\mathrm{SV}}$ = stillage valorization; $\mathbf{J}^{\mathrm{LV}}$ = lignin valorization; $\mathbf{J}^{\mathrm{WWT}}$ = wastewater treatment; $\mathbf{J}^{\mathrm{CB}}$ = combustor and boiler; $\mathbf{J}^{\mathrm{TBG}}$= turbogenerator.

c) Port numbers $pn \in \mathbf{PN}$.
   - $\mathbf{PN}^{\mathrm{IN}}$: inlet port number; $\mathbf{PN}^{\mathrm{OUT}}$= outlet port number.

d) Ports $p \in \mathbf{P} \subset \mathbf{J} \times \mathbf{PN}$, which is indexed by block and port number.
   - $\mathbf{P}^{\mathrm{IN}}$: inlet ports; $\mathbf{P}^{\mathrm{OUT}}$: outlet ports; $\mathbf{P}_j^{\mathrm{IN}}$: inlet ports of block j; $\mathbf{P}_j^{\mathrm{OUT}}$: outlet ports of block j.

e) Streams $s \in \mathbf{S} \subset \mathbf{P} \times \mathbf{P}$, which is indexed by two ports.
   - $\mathbf{S}_{p'}$: streams originating from outlet port p'; $\mathbf{S}_j$: streams that are connected to block j.

The binary parameters $\chi_{i,p',p}$ can be predefined for the component i present in the stream from outlet port p' and inlet port p after the superstructure is generated. The examples of sets, subsets and binary parameters are shown in **Figure S2A**. For example, the stream between outlet port P3 and inlet port P5 does not contain component Cc, therefore $\chi_{\mathrm{Cc,P3,P5}} = 0$.

The parameters are given as follows:

- λ_i: unit price of components $i \in \mathbf{I}^{\mathrm{F}} \cup \mathbf{I}^{\mathrm{R}} \cup \mathbf{I}^{\mathrm{P}} \cup \mathbf{I}^{\mathrm{B}}$ (\$ kg^{-1} or \$ kWh^{-1}).
- $\underline{\varrho}_i / \overline{\varrho}_i$: minimum/maximum supply of components $i \in \mathbf{I}^{\mathrm{F}} \cup \mathbf{I}^{\mathrm{R}}$ (kg or kWh).
- $\underline{\rho}_i / \overline{\rho}_i$: minimum/maximum demand of components $i \in \mathbf{I}^{\mathrm{P}} \cup \mathbf{I}^{\mathrm{B}}$ (kg or kWh).
- $\underline{\zeta}_j / \overline{\zeta}_j$: lower/upper capacity bounds of block j (kg or kWh).

- $\mu_{i,j}$: unit energy $i \in \mathbf{I}^{\mathrm{E}}$ (heat and electricity) requirement of block j (kWh kg^{-1}).
- $\eta_{i,p,i',p'}$: conversion coefficient (kg kg^{-1} or kWh kg^{-1} or kWh kWh^{-1}).
- θ_j: unit production cost of block j (\$ kg^{-1} or \$ kWh^{-1}).
- κ: boiler efficiency.

Variable $Y_j \in \{0,1\}$, which is equal to 1 if block j is selected, and the following nonnegative continuous variables are introduced:

- $E^{\mathrm{C}}_{i\,p',p}$: energy flow between outlet port p' and inlet port p (kWh).
- $E^{\mathrm{IN}}_{i,p}/E^{\mathrm{OUT}}_{i,p'}$: inlet/outlet energy flow (kWh).
- $E^{\mathrm{SR}}_{i}/E^{\mathrm{SK}}_{i}$: energy flow from/towards source/sink (kWh).
- $E^{\mathrm{UT}}_{i}/E^{\mathrm{W}}$: total energy requirement of biorefinery/waste heat (kWh).
- $F^{\mathrm{C}}_{i,\,p',p}$: mass flow between outlet port p' and inlet port p (kg).
- $F^{\mathrm{IN}}_{i,p}/F^{\mathrm{OUT}}_{i,p'}$: inlet/outlet mass flow (kg).
- $F^{\mathrm{SR}}_{i}/F^{\mathrm{SK}}_{i}$: mass flow from/towards source/sink (kg).
- $R_{p',p}$: split fraction of stream between outlet port p' and inlet port p.
- X_j: total consumption level of block j (kg).
- Z: total cost (\$).

Material Balance

The feedstock flow is converted into flows of the major constituent of biomass (e.g., glucan, xylan, and lignin) through a dummy conversion block (**Figure S2B**) modeled as follows:

$$\sum_{i\in\mathbf{I}^{\mathrm{F}}} \eta_{i,p''=\mathrm{DFI},i',p'=\mathrm{DFO}} F^{\mathrm{SR}}_{i} = \sum_{j\in\mathbf{J}^{\mathrm{PRE}},p\in\mathbf{P}^{\mathrm{IN}}_{j}} F^{\mathrm{C}}_{i',p'=\mathrm{DFO},p} \qquad \forall i' \in \mathbf{I}^{\mathrm{I}} \tag{1}$$

where $\eta_{i,p'',i',p'}$ in this equation corresponds to the composition of biomass feedstock. DFI and DFO are dummy inlet port and outlet port, respectively (see **Figure S2B**).

The inlet mass flow $F^{\mathrm{IN}}_{i,p}$ (**Figure S2C**) is given as:

$$F^{\mathrm{IN}}_{i,p} = \sum_{p'\in\mathbf{P}^{\mathrm{OUT}}|\chi_{i,p',p}=1} F^{\mathrm{C}}_{i,\,p',p} \qquad \forall i \in \mathbf{I}^{\mathrm{I}}, j \in \mathbf{J} \setminus \mathbf{J}^{\mathrm{TBG}}, p \in \mathbf{P}^{\mathrm{IN}}_{j} \tag{2}$$

where $F^{\mathrm{C}}_{i,\,p',p}$ is the connecting flow between outlet and inlet ports.

The outlet mass flow $F^{\mathrm{OUT}}_{i',p'}$ is given as:

$$F^{\mathrm{OUT}}_{i',p'} = \sum_{i\in\mathbf{I}^{\mathrm{I}},p\in\mathbf{P}^{\mathrm{IN}}_{j}} \eta_{i,p,i',p'} F^{\mathrm{IN}}_{i,p} \qquad \forall i' \in \mathbf{I}^{\mathrm{I}}, j \in \mathbf{J} \setminus \left(\mathbf{J}^{\mathrm{CB}} \cup \mathbf{J}^{\mathrm{TBG}}\right), p' \in \mathbf{P}^{\mathrm{OUT}}_{j} \tag{3}$$

where $\eta_{i,p,i',p'}$ is a conversion coefficient.

The outlet mass flow is split at the outlet port:

$$F^{\mathrm{OUT}}_{i,p'} = \sum_{p\in\mathbf{P}^{\mathrm{IN}}|\chi_{i,p',p}=1} F^{\mathrm{C}}_{i,\,p',p} \qquad \forall i \in \mathbf{I}^{\mathrm{I}}, j \in \mathbf{J} \setminus \left(\mathbf{J}^{\mathrm{CB}} \cup \mathbf{J}^{\mathrm{TBG}}\right), p' \in \mathbf{P}^{\mathrm{OUT}}_{j} \tag{4}$$

The split fraction $R_{p',p}$ is introduced to denote the fraction of stream leaving outlet port p' and entering inlet port p to ensure that the component concentrations in all outgoing streams are the same:

$$F_{i,p'}^{\mathrm{OUT}} R_{p',p} = F_{i,p',p}^{\mathrm{C}} \qquad \forall i \in \mathbf{I}^{\mathrm{I}}, p', p | \chi_{i,p',p} = 1 \tag{5}$$

$R_{p,p'}$ is constrained by the following equations:

$$0 \le R_{p',p} \le Y_j \qquad \forall j, (p', p) \in \mathbf{S}_j \tag{6}$$

$$\sum_{p \in \mathbf{S}_{p'}} R_{p',p} = Y_j \qquad \forall j, p' \in \mathbf{P}_j^{\mathrm{OUT}} \tag{7}$$

where Y_j is the binary variable for the selection of block j.

The mass inflow towards sink (e.g., product and by-product) F_i^{SK} is given as:

$$F_i^{\mathrm{SK}} = \sum_{p' \in \mathbf{P}^{\mathrm{OUT}} | \chi_{i,p',p=\mathrm{DPBI}}=1} F_{i,p',p=\mathrm{DPBI}}^{\mathrm{C}} \qquad \forall i \in \mathbf{I}^{\mathrm{P}} \cup \mathbf{I}^{\mathrm{B}} \tag{8}$$

where DPBI is the dummy inlet port of a dummy conversion block (see **Figure S2D**).

Additional resources (e.g., natural gas) can also be fed to the CB blocks (see **Figure S2E**):

$$F_i^{\mathrm{SR}} = \sum_{j \in \mathbf{J}^{\mathrm{CB}}, p \in \mathbf{P}_j^{\mathrm{IN}}} F_{i,p}^{\mathrm{IN}} \qquad \forall i \in \mathbf{I}^{\mathrm{R}} \tag{9}$$

Energy Balance

The heat generated from the CB blocks $E_{i'=\mathrm{heat},p'}^{\mathrm{OUT}}$ is given as:

$$E_{i'=\mathrm{heat},p'}^{\mathrm{OUT}} = \sum_{i \in \mathbf{I}^{\mathrm{I}} \cup \mathbf{I}^{\mathrm{R}}, p \in \mathbf{P}_j^{\mathrm{IN}}} \eta_{i,p,i'=\mathrm{heat},p'} F_{i,p}^{\mathrm{IN}} \qquad \forall j \in \mathbf{J}^{\mathrm{CB}}, p' \in \mathbf{P}_j^{\mathrm{OUT}} \tag{10}$$

After considering boiler efficiency κ, the heat balance is:

$$\kappa E_{i=\mathrm{heat},p'}^{\mathrm{OUT}} = E_{i=\mathrm{heat}}^{\mathrm{UT}} + E^{\mathrm{W}} + \sum_{p \in \mathbf{P}^{\mathrm{IN}} | \chi_{i=\mathrm{heat},p',p}=1} E_{i=\mathrm{heat},p',p}^{\mathrm{C}} \quad \forall j \in \mathbf{J}^{\mathrm{CB}}, p' \in \mathbf{P}_j^{\mathrm{OUT}} \tag{11}$$

where E_i^{UT} is the total energy (heat/electricity) requirement at the biorefinery; E^{W} is waste heat if no turbogenerator is selected; $E_{i,p',p}^{\mathrm{C}}$ is the connecting energy flow between two ports. E_i^{UT} is determined in the following equation:

$$E_i^{\mathrm{UT}} = \sum_j \mu_{i,j} X_j \qquad \forall i \in \mathbf{I}^{\mathrm{E}} \tag{12}$$

where $\mu_{i,j}$ is the unit energy requirement of each block j and X_j is the total consumption level of block j, which is given as:

$$X_j = \sum_{i \in \mathbf{I}^{\mathrm{I}} \cup \mathbf{I}^{\mathrm{R}} \setminus \mathbf{I}^{\mathrm{E}}, p \in \mathbf{P}_j^{\mathrm{IN}}} F_{i,p}^{\mathrm{IN}} \qquad \forall j \in \mathbf{J} \setminus \mathbf{J}^{\mathrm{TBG}} \tag{13}$$

$$X_j = \sum_{i \in \mathbf{I}^{\mathrm{E}}, p \in \mathbf{P}_j^{\mathrm{IN}}} E_{i,p}^{\mathrm{IN}} \qquad \forall j \in \mathbf{J}^{\mathrm{TBG}} \tag{14}$$

The heat inlet flow at the TBG blocks $E_{i,p}^{\mathrm{IN}}$ (**Figure S2E**) is given as:

$$E_{i=\mathrm{heat},p}^{\mathrm{IN}} = \sum_{p' \in \mathbf{P}^{\mathrm{OUT}} | \chi_{i=\mathrm{heat},p',p}=1} E_{i=\mathrm{heat},p',p}^{\mathrm{C}} \qquad \forall j \in \mathbf{J}^{\mathrm{TBG}}, p \in \mathbf{P}_j^{\mathrm{IN}} \tag{15}$$

The electricity generated by the TBG block $E_{i=\mathrm{electricity},p'}^{\mathrm{OUT}}$ is given as:

$$E^{\mathrm{OUT}}_{i'=\mathrm{electricity},p'} = \sum_{p\in \mathbf{P}_j^{\mathrm{IN}}} \eta_{i=\mathrm{heat},p,i'=\mathrm{electricity},p'} E^{\mathrm{IN}}_{i=\mathrm{heat},p} \qquad \forall j \in \mathbf{J}^{\mathrm{TBG}}, p' \in \mathbf{P}_j^{\mathrm{OUT}} \tag{16}$$

The electricity balance is given as:

$$\sum_{j\in \mathbf{J}^{\mathrm{TBG}},p'\in \mathbf{P}_j^{\mathrm{OUT}}} E^{\mathrm{OUT}}_{i=\mathrm{electricity},p'} + E^{\mathrm{SR}}_{i=\mathrm{electricity}} = E^{\mathrm{UT}}_{i=\mathrm{electricity}} + E^{\mathrm{SK}}_{i=\mathrm{electricity}} \tag{17}$$

where electricity E_i^{SR} and E_i^{SK} can be purchased and sold from and to the market, respectively.

Bounds

The product and by-product are bounded as follows:

$$\underline{\rho}_i \le F_i^{\mathrm{SK}} \le \overline{\rho}_i \qquad \forall i \in \mathbf{I}^{\mathrm{P}} \cup \mathbf{I}^{\mathrm{B}} \setminus \mathbf{I}^{\mathrm{E}} \tag{18}$$

$$\underline{\rho}_i \le E_i^{\mathrm{SK}} \le \overline{\rho}_i \qquad \forall i \in \mathbf{I}^{\mathrm{B}} \cap \mathbf{I}^{\mathrm{E}} \tag{19}$$

Similarly, the feedstock and resource flows are bounded as follows:

$$\underline{\varrho}_i \le F_i^{\mathrm{SR}} \le \overline{\varrho}_i \qquad \forall i \in \mathbf{I}^{\mathrm{F}} \cup \mathbf{I}^{\mathrm{R}} \setminus \mathbf{I}^{\mathrm{E}} \tag{20}$$

$$\underline{\varrho}_i \le E_i^{\mathrm{SR}} \le \overline{\varrho}_i \qquad \forall i \in \mathbf{I}^{\mathrm{R}} \cap \mathbf{I}^{\mathrm{E}} \tag{21}$$

The consumption level is bounded by:

$$\underline{\zeta}_j Y_j \le X_j \le \overline{\zeta}_j Y_j \qquad \forall j \tag{22}$$

The following constraints enforce the number of blocks to be selected:

$$\sum_{j\in \boldsymbol{J}^{\mathrm{PRE}}} Y_j = 1, \sum_{j\in \boldsymbol{J}^{\mathrm{HYD}}} Y_j \le 1, \sum_{j\in \boldsymbol{J}^{\mathrm{FER}}} Y_j = 1, \sum_{j\in \boldsymbol{J}^{\mathrm{SEP}}} Y_j = 1, \sum_{j\in \boldsymbol{J}^{\mathrm{WWT}}} Y_j = 1, \sum_{j\in \boldsymbol{J}^{\mathrm{CB}}} Y_j = 1 \tag{23}$$

Objective Function

The objective is to minimize the total cost, which includes the feedstock and additional resource purchases, and the total production cost of the biorefinery, minus the sales of by-products.

$$\mathrm{Min}\ Z = \left(\sum_{i\in \mathbf{I}^{\mathrm{F}}\cup \mathbf{I}^{\mathrm{R}}\setminus \mathbf{I}^{\mathrm{E}}} \lambda_i F_i^{\mathrm{SR}} + \sum_{i\in \mathbf{I}^{\mathrm{R}}\cap \mathbf{I}^{\mathrm{E}}} \lambda_i E_i^{\mathrm{SR}}\right) + \sum_j \theta_j X_j - \left(\sum_{i\in \mathbf{I}^{\mathrm{B}}\setminus \mathbf{I}^{\mathrm{E}}} \lambda_i F_i^{\mathrm{SK}} + \sum_{i\in \mathbf{I}^{\mathrm{B}}\cap \mathbf{I}^{\mathrm{E}}} \lambda_i E_i^{\mathrm{SK}}\right) \tag{24}$$

where λ_i is the unit price of components i and θ_j is the unit production cost of blocks j.

Note that the formulations are linear, except the bilinearities in Equation 5. The MINLP model is implemented in GAMS and solved using BARON.

Impact of Uncertainty: Major Parameters Not Describing Lignin Valorization

We study the impact of uncertainty in four parameters (feedstock price, electricity price, production cost, and lignin conversion coefficient in pretreatment) on the ethanol production cost in the base case design (S^{BC}). Specifically, we calculate the cost for 5,000 randomly generated scenarios, where, in each scenario, a value for each one of these four parameters is sampled from the corresponding (triangular) distribution. The assumptions for these distributions are taken from: (A) Feedstock price (Huang et al., 2018), (B) electricity export price (2002-2018 United States industrial average retail price of electricity from U.S. Energy Information Administration), (C) Production cost variation (Merrow et al., 1981), and (D) Lignin conversion coefficient in GVL block (Won et al., 2017). The parameters of the distributions as well as the histograms of the values used in our evaluation are shown in **Figure S3**. The optimization model is run for each one of the scenarios, and the distribution of the resulting minimum ethanol cost is shown in **Figure S4**.

The distribution in **Figure S4** suggests that the impact of uncertainty in these parameters on the minimum ethanol cost is substantial. However, this does not mean that the insights, based on the strategy transitions shown in the heat maps in the paper, will change. This is because, as explained in the main text, changes in the four parameters studied here impact both the lignin-to-heat/power and lignin-to-bioproducts strategies.

To illustrate, consider uncertainty in pretreatment (which is one of the most challenging and expensive processing steps for lignocellulosic biomass). An increase in the pretreatment cost will not necessarily change the transition of configurations shown in our figures because more expensive pretreatment means a more expensive lignin stream, regardless of where this lignin stream goes (boiler vs. valorization). It will change the minimum cost of ethanol, that is, the scale of the shown heat maps, but it will not significantly change the actual selection of the lignin valorization block, which is what we aim to study primarily. More generally, uncertainty in the processing parameters (cost, conversion, energy requirement) of almost all blocks, other than lignin valorization, is expected to have, similarly, low impact. There are two exceptions: parameters describing the conversion of lignin to (1) heat and power, and (2) valuable chemicals.

The presented analysis can be viewed as a study of a basic trade-off: benefit from using lignin to produce heat and power (current configuration) *versus* benefit from valorizing lignin. Thus, it is the uncertainty in blocks CB, TBG, LV (see **Figure 1**) that will indeed change the results. However, combustion and electricity generation from steam are well known processes and the parameters we use have little uncertainty. Thus, it the uncertainty in lignin valorization, which is at early stages of development and hence subject to significant uncertainty, that is likely to change the selection of the optimal biorefinery strategy and economics. The analysis of the paper can be viewed, precisely, as a study of the impact of uncertainty in some key LV parameters. The heat maps show how the cost and biorefinery configurations change as the values of these uncertain parameters change.

Supplemental References

Aden, A., Ruth, M., Ibsen, K., Jechura, J., Neeves, K., Sheehan, J., Wallace, B., Montague, L., Slayton, A., Lukas, J., 2002. Lignocellulosic Biomass to Ethanol Process Design and Economics Utilizing Co-Current Dilute Acid Prehydrolysis and Enzymatic Hydrolysis for Corn Stover. Golden, CO (United States).

Bhalla, A., Fasahati, P., Particka, C.A., Assad, A.E., Stoklosa, R.J., Bansal, N., Semaan, R., Saffron, C.M., Hodge, D.B., Hegg, E.L., 2018. Integrated experimental and technoeconomic evaluation of two-stage Cu-catalyzed alkaline-oxidative pretreatment of hybrid poplar. Biotechnol. Biofuels 11, 143. https://doi.org/10.1186/s13068-018-1124-x

Da Costa Sousa, L., Jin, M., Chundawat, S.P.S., Bokade, V., Tang, X., Azarpira, A., Lu, F., Avci, U., Humpula, J., Uppugundla, N., Gunawan, C., Pattathil, S., Cheh, A.M., Kothari, N., Kumar, R., Ralph, J., Hahn, M.G., Wyman, C.E., Singh, S., Simmons, B.A., Dale, B.E., Balan, V., 2016. Next-generation ammonia pretreatment enhances cellulosic biofuel production. Energy Environ. Sci. 9, 1215–1223. https://doi.org/10.1039/c5ee03051j

Huang, K., Won, W., Barnett, K.J., Brentzel, Z.J., Alonso, D.M., Huber, G.W., Dumesic, J.A., Maravelias, C.T., 2018. Improving economics of lignocellulosic biofuels: An integrated strategy for coproducing 1,5-pentanediol and ethanol. Appl. Energy 213, 585–594. https://doi.org/10.1016/j.apenergy.2017.11.002

Humbird, D., Davis, R., Tao, L., Kinchin, C., Hsu, D., Aden, A., Schoen, P., Lukas, J., Olthof, B., Worley, M., Sexton, D., Dudgeon, D., 2011. Process Design and Economics for Biochemical Conversion of Lignocellulosic Biomass to Ethanol: Dilute-Acid Pretreatment and Enzymatic Hydrolysis of Corn Stover, National Renewable Energy Laboratory (NREL). Golden, CO (United States). https://doi.org/10.2172/1013269

Kazi, F.K., Fortman, J.A., Anex, R.P., Hsu, D.D., Aden, A., Dutta, A., Kothandaraman, G., 2010. Techno-economic comparison of process technologies for biochemical ethanol production from corn stover. Fuel 89, S20–S28. https://doi.org/10.1016/j.fuel.2010.01.001

Merrow, E.W., Phillips, K., Myers, C.W., 1981. Understanding Cost Growth and Performance Shortfalls in Pioneer Process Plants. RAND Corporation, Santa Monica, CA.

Ng, R.T.L., Fasahati, P., Huang, K., Maravelias, C.T., 2019. Utilizing stillage in the biorefinery: Economic, technological and energetic analysis. Appl. Energy 241, 491–503. https://doi.org/10.1016/j.apenergy.2019.03.020

Won, W., Motagamwala, A.H., Dumesic, J.A., Maravelias, C.T., 2017. A co-solvent hydrolysis strategy for the production of biofuels: Process synthesis and technoeconomic analysis. React. Chem. Eng. 2, 397–405. https://doi.org/10.1039/c6re00227g

Wu, W.Z., Henao, C.A., Maravelias, C.T., 2016. A superstructure representation, generation, and modeling framework for chemical process synthesis. AIChE J. 62, 3199–3214. https://doi.org/10.1002/aic.15300